

# Eu<sup>3+</sup> Complex/Polyimide Nanocomposites: Improvement in Mechanical and Thermal Properties

Li-Juan Bian, Xue-Feng Qian, Jie Yin, Zi-Kang Zhu, Qing-Hua Lu

Research Institute of Polymer Materials, School of Chemistry and Chemical Technology, Shanghai Jiao Tong University, Shanghai 200240, China

Received 20 August 2001; accepted 26 March 2002

**ABSTRACT:** A series of Eu<sup>3+</sup>-doped polyimide nanocomposites were successfully prepared via the solution process. X-ray diffraction, differential scanning calorimetric analysis, thermogravimetric analysis, transmission electron microscopic analysis, universal testing, and ellipsometry were used to characterize the nanocomposites. TEM results indicated that rare earth particles were homogeneously dispersed in the polyimide matrix with a size of about 20 nm. The introduction of the rare earth complex led to an increase

in the glass transition temperature, thermal stability, size stability, and a marked increase in the tensile strength and storage modulus. The addition of the rare earth complex also increased the refractive index of the nanocomposites. © 2002 Wiley Periodicals, Inc. *J Appl Polym Sci* 86: 2707–2712, 2002

**Key words:** nanocomposites; polyimides; inorganic materials

## INTRODUCTION

The property improvement of polymers via the homogenous incorporation of metallic salts and organometallic complexes within a polymer matrix is being actively pursued.<sup>1–5</sup> Various metallic salts and organometallic complexes were synthesized and many polymers were used as the matrix. The challenges in this area of high-performance organic–inorganic hybrid materials come from the need for significant improvements in the interfacial adhesion between the polymer matrix and the reinforcing material because the organic matrix is relatively incompatible with the inorganic phase. Nanocomposite is a class of composites in which the reinforcing phase dimensions are on the order of nanometers.<sup>6,7</sup> Because of their nanometer size characteristics, nanocomposites possess superior properties over the conventional microcomposites because of the strong interfacial adhesion. In recent years, polymers containing inorganic nanoparticles have been the focus of much research.<sup>8–10</sup>

Polyimides are a type of high-performance polymers widely applied in various industries because of their outstanding chemical resistance, mechanical properties, electrical properties, and radiation resistance, especially at elevated temperature. Recently, polyimide-containing inorganic nanoparticles has at-

tracted a lot of attention.<sup>11–15</sup> However, the reports on the polyimide-containing rare earth ions are limited. Southward et al. have worked on the hybrid system of fluorinated polyimide doped by lanthanide ions.<sup>11,16–18</sup> The results showed that the incorporation of lanthanide complexes could effectively lower the coefficient of thermal expansion (CTE).

In this study, we prepared europium (III)/polyimide hybrids. The polyimide was based on two conventional monomers: benzophenone-3,3',4,4'-tetracarboxylic dianhydride (BTDA) and 4,4'-oxydianiline (ODA) (the chemical structure is shown in Scheme 1). Soluble europium (III) pyridine carboxylic acid was used as the inorganic phase. It was found, apart from the obvious reduction of the CTE, that the mechanical and thermal properties were also effectively improved.

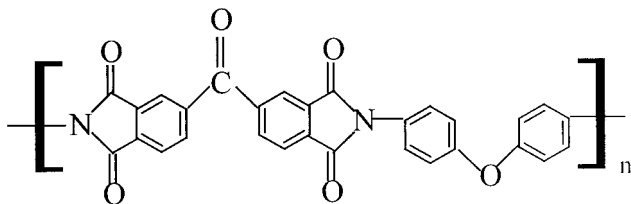
## EXPERIMENTAL

### Materials

BTDA was prepared from benzophenone-3,3',4,4'-tetracarboxylic acid (industrial product, purchased from Beijing Tar Chemical Co.) by refluxing with an excessive amount of acetic anhydride for 2 h. ODA (analytical reagent grade, purchased from Shanghai Chemical Reagent Co.) was recrystallized from ethanol before use. Eu<sub>2</sub>O<sub>3</sub> (99.99 wt %, purchased from Shanghai Yao Long Non-Ferrous Metals Ltd.) and pyridine carboxylic acid (analytical reagent grade, purchased from Shanghai Chemical Reagent Co.) were used as received. Other common chemical reagents were used without purification.

Correspondence to: Z.-K. Zhu (lmsun@mail.sjtu.edu.cn).

Contract grant sponsor: Shanghai Jiao Tong University Foundation of Natural Science Research.



Scheme 1 Structure of polyimide.

### Synthesis of rare earth complex—EuL<sub>3</sub>·2H<sub>2</sub>O (L = pyridine carboxylic acid)

EuL<sub>3</sub>·2H<sub>2</sub>O was prepared from Eu<sub>2</sub>O<sub>3</sub>, pyridine carboxylic acid, and NaOH, according to ref. <sup>19</sup>. First, pyridine carboxylic acid (3 mmol) was dissolved in 20 mL hot water, and 4 mol/L NaOH aqueous solution was then added under efficient agitation until the pH of solution (L solution) was about 6. Europium chloride (1 mmol), which was prepared from Eu<sub>2</sub>O<sub>3</sub> and hydrochloric acid, was dissolved in 10 mL water, and this solution was added dropwise to the L solution. The mixture was stirred at 70°C for 6 h and then cooled. The product was collected by filtration and washed with ethanol and water. For the simple, EuL<sub>3</sub>·2H<sub>2</sub>O was simplified EuL<sub>3</sub>.

### Preparation of EuL<sub>3</sub>/polyimide hybrid materials

The condensation between ODA and BTDA in *N,N*-dimethylformamide (DMF) at room temperature gave a polyamic acid (PAA) solution. To this solution, an appropriate amount of solid EuL<sub>3</sub> was added. The mixture was stirred for 24 h to give a homogeneous solution. During the dissolution of EuL<sub>3</sub>, the viscosity of the mixture obviously increased, indicating that Eu(III) had coordinated to the polyamic acid molecules. The clear EuL<sub>3</sub>/PAA solution was cast on a glass substrate, which was washed with deionized water and ethanol before use. The cast film was kept for 16 h at 60°C to evaporate most of the solvent and

then thermally treated consecutively at 100, 120, 140, 160, 180, 220, and 270°C for 2 h for each of the temperatures to imidize PAA and remove the solvent thoroughly. The film was removed from the substrate by soaking in deionized water.

### Characterization

Thermogravimetric (TGA) and differential scanning calorimetric (DSC) analyses were performed on Perkin-Elmer TGA 7 and Pyris I DSC, respectively, in nitrogen with a scan rate of 20°C/min. The coefficients of thermal expansion (CTE) of the hybrid films were measured with Rheometric Scientific DMTA IV with a TMA mode. CTE was calculated over the range of 75–125°C. X-ray diffraction (XRD) patterns were recorded on D/max-RD X-ray diffraction spectrometer with a copper target at an operating voltage of 40 kV and an electric current of 100 mA. Mechanical properties were measured at ambient temperature on an Instron-4465 universal tester. The tensile properties of each sample were determined from an average of at least five tests. The storage moduli were measured with Rheometric Scientific DMTA IV with a DMA mode. Transmission electron microscopic (TEM) analysis was conducted on a Philips CM 120 TEM. Refractive indices of the hybrid films were measured on a Woollan VASE 32 ellipsometer.

## RESULTS AND DISCUSSION

The PI/EuL<sub>3</sub> hybrid containing 3 wt % EuL<sub>3</sub> was named PI/EuL<sub>3</sub>-3. Other samples were named accordingly.

### Structure and thermal stability of the rare earth complex, EuL<sub>3</sub>·2H<sub>2</sub>O

The EuL<sub>3</sub> complex is quite soluble in DMF and dimethyl sulfoxide (DMSO). The infrared spectrum of

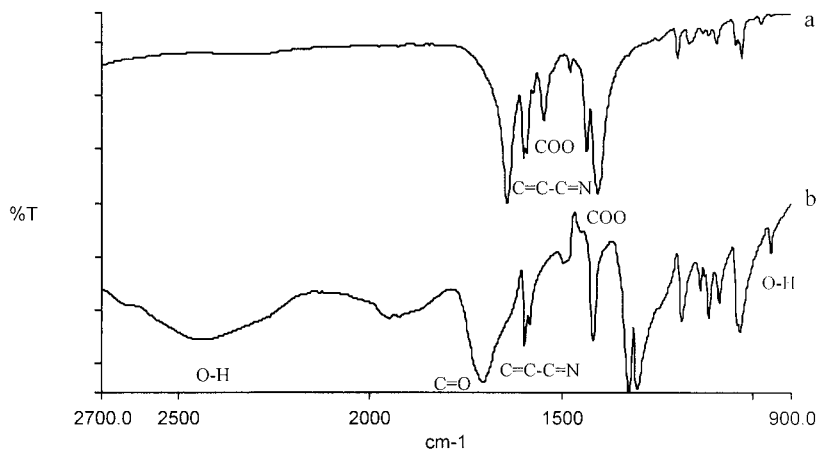
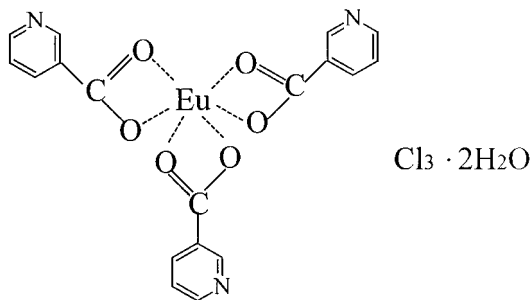


Figure 1 Infrared spectra of the rare earth complex (a) and ligand (b).



Scheme 2 Structure of  $\text{EuL}_3 \cdot 2\text{H}_2\text{O}$ .

the complex is shown in Figure 1. The three absorption peaks  $\nu_{\text{O-H}}$  ( $2200\text{--}2700\text{ cm}^{-1}$ ),  $\nu_{\text{C=O}}$  ( $1705\text{ cm}^{-1}$ ),  $\delta_{\text{O-H}}$  ( $952\text{ cm}^{-1}$ ) corresponding to the pyridine carboxylic acid were absent after the formation of the complex. The typical antisymmetric and symmetric stretching vibrations of pyridine carboxylic acid at about  $1546$  and  $1405\text{ cm}^{-1}$  were present. These results suggested that coordination bonds were formed between Eu(III) and O from the pyridine carboxylic acid. Compared to the obvious change in the absorption from the ligand, the backbone vibration peak ( $1595\text{ cm}^{-1}$ ) was almost unchanged after the formation of the complex, indicating that the nitrogen atoms from the ligand did not participate in the coordination. The structure of the complex is shown in Scheme 2. The results of elemental analysis are listed in Table I. The calculated value accorded well with the measured value, and it further verified the structure of rare earth complex (Scheme 2). The TGA curve (Fig. 2) of the  $\text{EuL}_3$  complex revealed two thermal decomposition steps. The first step, found at  $130\text{--}215^\circ\text{C}$ , was from the loss of the two molecules of water (from the calculation), and the second step began at about  $363^\circ\text{C}$ . This TGA result indicated that the rare earth complex had good thermal stability and should be stable during the thermal treatment process.

### Structure of PI/ $\text{EuL}_3$ composites

The X-ray diffraction patterns of the virgin and doped polyimide films are shown in Figure 3. Only one broad peak associated with the matrix polyimide was observed in both samples. Meanwhile, no crystalline calorimetric exotherms were found in their DSC curves (Fig. 7). Both results indicated that  $\text{EuL}_3$  existed in an amorphous state in the polyimide film.

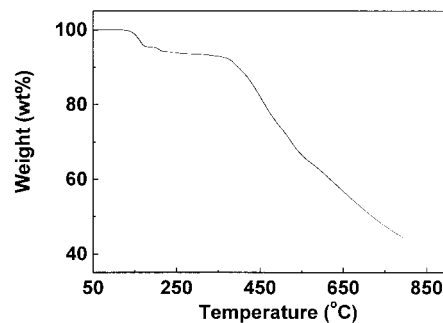


Figure 2 TGA curve of  $\text{EuL}_3$ .

Figure 4 shows the TEM photograph of PI/ $\text{EuL}_3$ -3 film, which reveals that  $\text{EuL}_3$  dispersed homogeneously in the hybrid with a particle size of about 20 nm. This good dispersion of  $\text{EuL}_3$  in PI was caused by the strong interaction between them, which limited the aggregation of  $\text{EuL}_3$ .

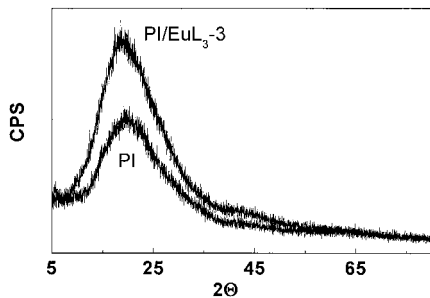
### Mechanical properties

Figure 5 shows that the introduction of a very small amount of  $\text{EuL}_3$  leads to a clear increase in the tensile strength of the composite films. Compared to the virgin PI, the introduction of 1 wt %  $\text{EuL}_3$  leads to an increase of 23% in tensile strength. The increase in the tensile strength reflects the reinforcement effect attained by the dispersion of  $\text{EuL}_3$  into polyimide film. Rare earth elements have great coordination numbers, and europium has a large coordination number of 12. Moreover, rare earth atoms are easy to coordinate with N and O atoms in polymer. There are many N and O atoms in polyimide and it is easy for  $\text{Eu}^{3+}$  to coordinate to the polyimide molecules. So, this increase in tensile strength was probably caused by the strong interaction between  $\text{EuL}_3$  and PI, which makes  $\text{EuL}_3$  act as a crosslink point. Because  $\text{EuL}_3$  was well dispersed in PI, only a small amount of  $\text{EuL}_3$  led to a large amount of crosslinking points. However, further increase in the  $\text{EuL}_3$  content caused a decrease in the tensile strength, probably because of the increased tendency of aggregation of  $\text{EuL}_3$ . The hybrid containing 3 wt %  $\text{EuL}_3$  had a similar tensile strength to the virgin PI.

The introduction of  $\text{EuL}_3$  also led to a linear increase in the storage modulus of the hybrid (Fig. 6). The introduction of only 3 wt %  $\text{EuL}_3$  led to a 73% increase

TABLE I  
Elemental Analysis of  $\text{EuL}_3 \cdot 2\text{H}_2\text{O}$

C (%)		H (%)		N (%)	
Calculated	Measured	Calculated	Measured	Calculated	Measured
32.70	32.10	2.42	2.73	6.35	6.30



**Figure 3** X-ray diffraction patterns of PI/EuL<sub>3</sub>-3 and virgin PI.

in the storage modulus on the basis of the virgin PI (from 1.4 to 2.4 GPa). This dramatic increase in the modulus was caused by the strong interaction between the EuL<sub>3</sub> and the PI, which limited the segmental movement of PI.

### Thermal properties

The strong interaction between EuL<sub>3</sub> and PI would also lead to an increase in the glass transition temperature of the composites, which was confirmed by their DSC curves (Fig. 7 and Table II). They showed that the  $T_g$ 's modestly increased with increased EuL<sub>3</sub> content.

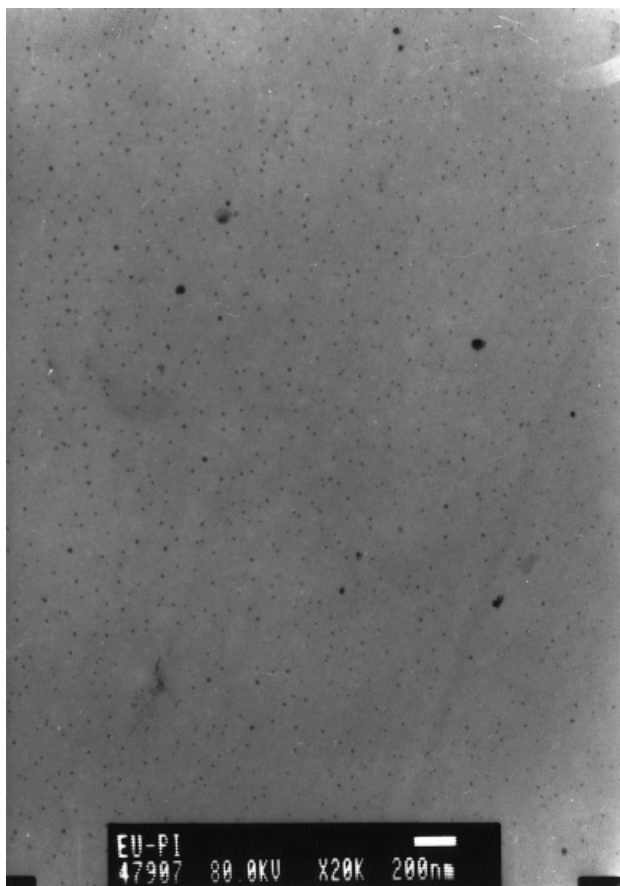


**Figure 4** TEM photograph of PI/EuL<sub>3</sub>-3.

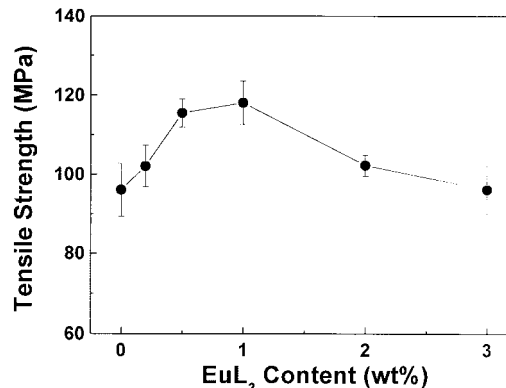


**Figure 5** Mechanical properties of PI/EuL<sub>3</sub> composite films.

The  $T_g$  was increased by 19.6°C when 3 wt % EuL<sub>3</sub> was introduced. Because the glass transition process is related to the molecular motion,<sup>20</sup> the strong interaction between EuL<sub>3</sub> and PI limits the cooperative motions of the polyimide main-chain segments.

Meanwhile, their TGA curves (Fig. 8) also revealed that the thermal stability of the hybrids was improved with the addition of EuL<sub>3</sub>. The temperatures at 10% weight loss ( $T_{10}$ ) are listed in Table II and showed a 16°C increase in  $T_{10}$  when only 3 wt % of EuL<sub>3</sub> was added. This may be due to the existence of the physical crosslink network caused by the strong interaction between EuL<sub>3</sub> and PI, and, to a certain extent, the increased europium residue at high temperature.

We also studied the thermal expansion behavior of the PI/EuL<sub>3</sub> composites with a temperature range of 75–125°C (see Table II). The CTE of the hybrids decreased with increasing EuL<sub>3</sub> content. The CTE decrease was 16.4% for a very low EuL<sub>3</sub> content (3%). This decrease in CTE was caused by the fine dispersion of EuL<sub>3</sub> and strong interaction between EuL<sub>3</sub> and PI, which limited the segmental movement of PI. The decrease in CTE (or increase in size stability) is extremely desirable for the matching of thermal expansion between PI and inorganic substrates (such as metals, glass, and silicon).

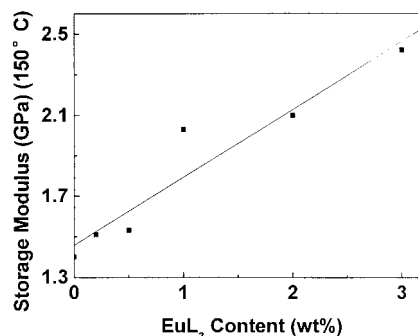


**Figure 6** Relationship between the EuL<sub>3</sub> content and storage modulus of PI/EuL<sub>3</sub> composite films.

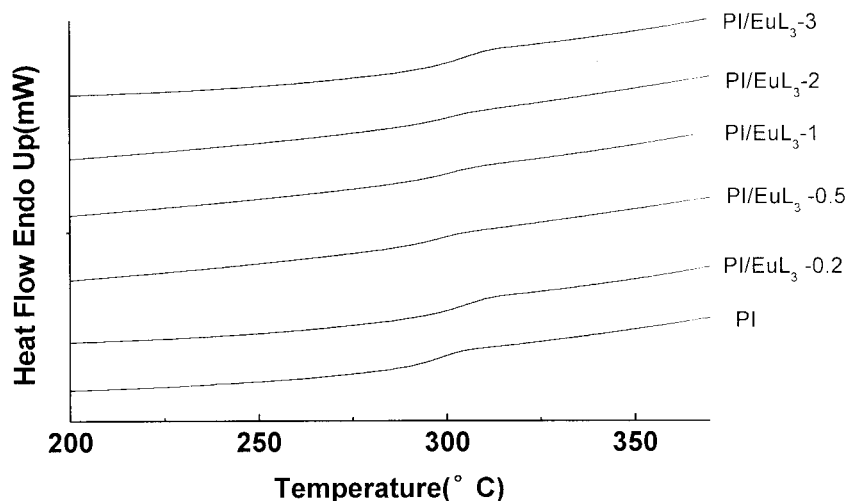


Figure 7 DSC curves of PI and PI/EuL<sub>3</sub> composites.

### Refractive index

Because atoms of a rare earth element are large and have great polarity, rare earth element containing materials usually have a high refractive index. From Figure 9 we also found that the introduction of EuL<sub>3</sub>

increased the refractive index of polyimide. When the EuL<sub>3</sub> content was 10 wt %, the refractive index of the hybrid was 1.7889 at 633 nm, much higher than that of the virgin PI (1.7086). The increase in the refractive index by the addition of EuL<sub>3</sub> may have

TABLE II  
Thermal Property of PI/EuL<sub>3</sub> Hybrids

	PI	PI/EuL <sub>3</sub> -0.2	PI/EuL <sub>3</sub> -0.5	PI/EuL <sub>3</sub> -1	PI/EuL <sub>3</sub> -2	PI/EuL <sub>3</sub> -3
$T_g$ (°C) <sup>a</sup>	298.3	299.4	302.3	304.1	307.0	317.9
$T_{10}$ (°C) <sup>b</sup>	563.2	569.9	571.4	573.7	576.7	579.7
CTE (10 <sup>-6</sup> /K) <sup>c</sup>	45.6	40.8	40.6	39.5	39.0	38.1

<sup>a</sup> Glass transition temperature measured with DSC under the protection of N<sub>2</sub> with a scan rate of 20°C/min.

<sup>b</sup> Temperature at 10% weight loss measured by TGA under the protection of N<sub>2</sub> with a scan rate of 20°C/min.

<sup>c</sup> Coefficient of linear thermal expansion measured with DMA with TMA mode.

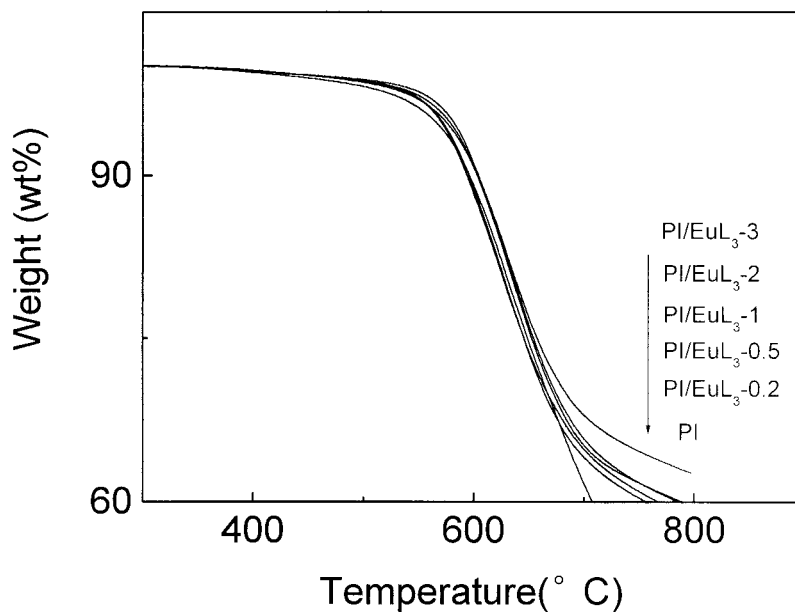


Figure 8 TGA curves of PI and PI/EuL<sub>3</sub> composites.

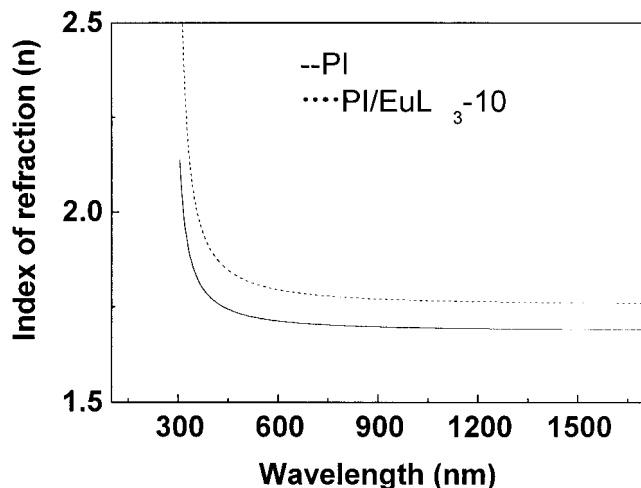


Figure 9 Index of refraction of PI and PI/EuL<sub>3</sub> composites.

potential application in optical and electronic devices.

### CONCLUSION

EuL<sub>3</sub>/PI hybrids have been successfully prepared. EuL<sub>3</sub> was very well dispersed in the PI matrix because of the strong interaction between EuL<sub>3</sub> and PI. The hybrids possess improved tensile strength and storage modulus, increased glass transition temperature, thermal stability, size stability, and refractive index compared to PI.

This work was financially supported by the Shanghai Jiao Tong University Foundation of Natural Science Research.

### References

- Zeng, H. M.; Zhang, Z. Y.; Wu, S. L. *Polymer* 1994, 35, 1092.
- Ellison, M. W.; Taylor, L. T. *Chem Mater* 1994, 6, 990.
- Sawada, T.; Ando, S. *Chem Mater* 1998, 10, 3368.
- Fu, L. S.; Zhang, H. J.; Wang, S. B.; Meng, Q. G.; Yang, K. Y.; Ni, J. Z. *J Sol-Gel Sci Tech* 1999, 15, 49.
- Kumar, R. V.; Diamant, Y.; Gedanken, A. *Chem Mater* 2000, 12, 2301.
- Novak, B. M. *Adv Mater* 1993, 5, 422.
- Frisch, H. L.; Mark, J. E. *Chem Mater* 1996, 8, 1735.
- Agag, T.; Koga, T.; Takeichi, T. *Polymer* 2001, 42, 3399.
- Huang, J. C.; Zhu, Z. K.; Qian, X. F.; Yin, J. *Mater Res Bull* 2000, 35, 2309.
- Giannelis, E. P. *Adv Mater* 1996, 8, 29.
- Southward, R. E.; Thompson, D. S.; Thornton, T. A.; Thompson, D. W.; St. Clair, A. K. *Chem Mater* 1998, 10, 486.
- Troger, L.; Hunnefeld, H.; Nunes, S.; Oehring, M.; Fritsch, D. *J Phys Chem B* 1997, 101, 1279.
- Fritsch, D.; Peinemann, K. V. *Catal Today* 1995, 25, 277.
- Fritsch, D.; Peinemann, K. V. *J Membr Sci* 1995, 99, 29.
- Nandi, M.; Conklin, J. A.; Salvati, L., Jr.; Sen, A. *Chem Mater* 1990, 2, 772.
- Southward, R. E.; Thompson, D. S.; Thompson, D. W.; St. Clair, A. K. *J Adv Mater* 1996, 27, 2.
- Thompson, D. S.; Southward, R. E.; St. Clair, A. K. *Polym Mater Sci Eng* 1994, 71, 725.
- Southward, R. E.; Thompson, D. S.; Thompson, D. W.; Thornton, T. A.; St. Clair, A. K. *Polym Mater Sci Eng* 1997, 76, 185.
- Xu, Z. D.; Wang, M.; Feng, D. Z. *Chinese J Appl Chem* 1999, 16, 18.
- Agag, T.; Koga, T.; Takeichi, T. *Polymer* 2001, 42, 3399.